Coordination of Alkali Metals to Oligosaccharides Dictates Fragmentation Behavior in Matrix Assisted Laser Desorption Ionization/Fourier Transform Mass Spectrometry

Mark T. Cancilla, Sharron G. Penn, James A. Carroll, and Carlito B. Lebrilla*

Contribution from the Department of Chemistry, University of California, Davis, California 95616

Received February 6, 1996[⊗]

Abstract: A correlation is found between the fragment ion yield and the degree of branching for oligosaccharides analyzed by matrix assisted laser desorption ionization/Fourier transform mass spectrometry (MALDI/FTMS). The most branched oligosaccharides produced the least amount of fragment ion. Another relationship is found between the size of the alkali metal ion and the yields of fragment ions. The smallest alkali metal ion produced the greatest amount of fragment ions. The presence of the quasimolecular ion is dependent on both the size of the metal ion and the size of the sugar. A minimum number of saccharide residues are necessary to stabilize the complex and produce a quasimolecular ion. Molecular mechanics calculations were performed and structures obtained consistent with the observed experimental behavior. The site of coordination plays a dominant role in the yield and types of fragment ions observed.

Introduction

The large number of isomeric structures possible with even small oligosaccharides make them extremely difficult to solve with any structural elucidation techniques. In mass spectrometry, the molecular mass and sequence fragments are not sufficient to fully characterize the primary structure. The presence of several linkage sites make possible numerous linkage combinations. Branching occurs when at least three monosaccharide units (monomers) are bonded to a single monomer. The determination of linkage type and the degree of branching can only be obtained if fragment ions are abundant. Cross-ring cleavages, two bond cleavages of the pyranose rings, are essential for providing linkage and branching information.

Mass spectrometry specifically with fast atom bombardment (FAB) and liquid secondary ion mass spectrometry (LSIMS) ionization methods have been extensively used to analyze oligosaccharides. The application and limitations of these two similar techniques are well-known and have been illustrated in several review and key articles.[1−27] Their major limitation is the relatively poor detection limit. Laser desorption, with and without, matrix has been more recently developed but has been used already with great success to analyze carbohydrate structures. Extensive fragementation is observed without matrix providing numerous structurally important fragment ions.[28−35] Laser desorption without matrix (LD) is unfortunately also limited by its relatively poor detection limits. Matrix assisted laser desorption ionization (MALDI) mass spectrometry is, in contrast, a highly sensitive method but often lacks the high degree of fragmentation necessary for the structural elucida-

[⊗] Abstract published in *Advance ACS Abstracts,* July 1, 1996.

(1) Orlando, R.; Bush, C. A.; Fenselau, C. *Biomed. Environ. Mass Spectrom.* **1990**, *19*, 747−54.
(2) Orlando, R.; Fenselau, C.; Cotter, R. J. *Anal. Chem.* **1990**, *62*, 2388−90.
(3) Dell, A.; Taylor, G. W. *Mass Spectrom. Rev.* **1984**, *3*, 357.
(4) Burlingame, A. L.; Baillie, T. A.; Derrick, P. J. *Anal. Chem.* **1986**, *58*, 165R.
(5) Burlingame, A. L.; Whitney, J. O.; Russel, D. H. *Anal. Chem.* **1984**,*56*, 417R.
(6) Montreuil, J. *Adv. Carbohydr. Chem. Biochem.* **1980**, *37*, 157.
(7) Puzo, G.; Prome, J. C. *Org. Mass Spectrom.* **1984**, *19*, 448−51.
(8) Aubagnac, J. L.; Devienne, F. M.; Combarieu, R. *Org. Mass. Spectrom.* **1983**, *18*, 361−4.
(9) Barofsky, D. F.; Giessman, U.; Barofsky, E. *Int. J. Mass Spectrom. Ion Phys.* **1983**, *53*, 319−22.
(10) Bosso, C.; Defaye, J.; Heyraud, A.; Ulrich J. *Carbohydr. Res.* **1984**, *125*, 309−17.
(11) Reinhold, V. N.; Carr, S. A. *Mass Spectrom. Rev.* **1983**, *2*, 153−221.
(12) Domon, B.; Costello, C. E. *Glycoconjugate J.* **1988**, *5*, 397−409.
(13) Domon, B.; Costello, C. E. *Biochemistry* **1988**, *27*, 1534−43.
(14) Guevremont, R.; Wright, J. L. C. *Rapid Commun. Mass Spectrom.* **1988**, *2*, 50−3.
(15) Laine, F. A.; Pamidimukkala, K. M.; French, A. D.; Hall, R. W.; Abbas, S. A.; Jain, R. K.; Matta, K. L. *J. Am. Chem. Soc.* **1988**, *110*, 6931−9.
(16) Zhou, Z.; Ogden, S.; Leary, J. A. *J. Org. Chem.* **1990**, *55*, 5444−6.
(17) Tondeur, Y.; Clifford, A. J.; DeLuca, L. M. *Org. Mass Spectrom.* **1985**, *20*, 157−60.
(18) Carroll, J. A.; Ngoka, L.; McCullough, S. M.; Gard, E.; Jones, A. D.; Lebrilla, C. B. *Anal. Chem.* **1991**, *63*, 2526−9.
(19) Dallinga, J. W.; Heerma, W. *Biol. Mass Spectrom.* **1991**, *20*, 215−31.
(20) Ngoka, L. C.; Gal, J. F.; Lebrilla, C. B. *Anal. Chem.* **1994**, *66*, 692−8.
(21) Lemoine, J.; Fournet, B.; Despeyroux, D.; Jennings, K. R.; Rosenberg, R.; Hoffman, E. d. *J. Am. Soc. Mass Spectrom.* **1993**, *4*, 197−203.
(22) Martin, W. B.; Silly, L.; Murphy, C. M.; T. J. Raley, J.; Cotter, R. J. *Int. J. Mass Spectrom. Ion Processes* **1989**, *92*, 243−65.
(23) Dell, A. *Adv. Carbohydr. Chem. Biochem.* **1987**, *45*, 19−72.
(24) Guevremont, R.; Wright, J. L. C. *Rapid Commun. Mass Spectrom.* **1987**, *1*, 12−3.
(25) Hemling, M. E.; Yu, R. K.; Sedgwick, R. D.; Rinehart, K. L. *Biochemistry* **1987**, *23*, 5706−13.
(26) Hounsell, E. F.; Madigan, M. J.; Lawson, A. M. *Biochem. J.* **1984**, *219*, 947−52.
(27) Teesch, L. M.; Adams, J. *Org. Mass Spectrom.* **1992**, *27*, 931−43.
(28) Coates, M. L.; Wilkins, C. L. *Anal. Chem.* **1987**, *59*, 197.
(29) Coates, M. L.; Wilkins, C. L. *Biomed. Mass Spectrom.* **1985**, *12*, 424.
(30) Spengler, B.; Dolce, J. W.; Cotter, R. J. *Anal. Chem.* **1990**, *62*, 1731−7.
(31) Roczko, A. W.; Viswanadham, S. K.; Sharkey, A. G.; Hercules, D. M. *Fesenius Z. Anal. Chem.* **1989**, *334*, 521−6.
(32) Stahl, B.; Steup, M.; Karas, M.; Hillenkamp, F. *Anal. Chem.* **1991**, *63*, 1463−6.
(33) Lam, Z.; Comisarow, M. B.; Dutton, G. G. S.; Parolis, H.; Parolis, L. A. S.; Bjarnason, A.; Weil, D. A. *Anal. Chim. Acta* **1990**, *241*, 187−99.
(34) Lam, Z.; Comisarow, M. B.; Dutton, G. G. S. *Anal. Chem.* **1988**, *60*, 2304.
(35) Lam, Z.; Comisarow, M. B.; Dutton, G. G. S.; Weil, D. A. *Rapid. Commun. Mass Spectrom.* **1987**, *1*, 83.

S0002-7863(96)00376-9 CCC: $12.00

tion.[32] In time-of-flight (TOF) instruments, techniques such as post-source decay (PSD) are used to produce a greater fragment ion yield.[36] PSD delays the detection of ions, on the microsecond time scale, to allow metastable dissociation to occur. Alternatively, in Fourier transform mass spectrometry (FTMS), the detection delay times are in the order of 10^{-3} to 10^{2} s, sufficient to allow metastable ions to dissociate. In addition, FTMS provides capabilities not readily obtained by other MS techniques such as ultrahigh resolution (10^{6} at $m/z > 5000$) and accurate mass (<5 ppm at up to m/z 2000).[37−39] The combination of MALDI/FTMS should therefore be extremely useful for the elucidation of carbohydrate structures from the standpoint of sensitivity and fragment ion yield.

Although oligosaccharides have not been as widely studied as peptides with MALDI, the method has been shown to be highly effective in characterizing unknown compounds.[32,36,40−49] Two major factors are expected in MALDI to affect the yield of fragment ions: the laser and the matrix. The wavelength, the laser fluences, angle of incidence, and laser focus size are all known to affect the yield of ions.[50−52] The use of different matrices, co-matrices, and additives also varies that yield.[32,48] For oligosaccharides, 2,5-dihydroxybenzoic acid is emerging as the best matrix, providing good sensitivity and allowing quantification of mixtures,[32,48,53] although the use of co-matrices appears promising.[43,54] In the spectra, the quasimolecular ion is always the sodiated species unlike peptides where the protonated species usually dominates. Chemical factors related to the analyte ion, such as structure and the coordinating metal, are expected to also affect the yield of fragment ions. Given the relationship between detect time and fragment ion yield, these factors may be greatly enhanced in FTMS as compared to TOF mass spectrometry.

The effects of structures and coordinating metal ion on fragment ion yield in MALDI have not been directly or systematically studied. It is commonly understood that structure will affect the fragmentation pattern but the relationship between, for example, branching and fragment ion yield if it exists is not known. On other hand, the amount of branching in oligosaccharides has important significance in their biology. In high mannose sugars, for example, a higher amount of branching is found in cancerous cells compared to normal cells.[55,56]

There have been a dearth of studies to observe the affect of alkali metal ions on the MALDI/MS spectrum. A recent report by Mohr *et al*. suggests that based on the relative abundance of alkali metal doped maltoheptaose, the order of binding affinities for carbohydrates is as follows: H ≪ Li < Na < Ka < Cs.[43] A possible reason for the small number of these types of studies is that use of salts is often avoided in MALDI as it significantly complicates the mass spectra. In MALDI/FTMS we find that by varying the alkali metal ion concentration, we can suppress all other quasimolecular ions in favor of the coordinated metal from the dopant salt. In this study, we examine the relationship between branching and fragment ion yield during MALDI and explore the role of the alkali metal ion in promoting dissociation reactions during the MALDI process. Structures of the branched oligosaccharides used in this study are shown in Chart 1. The alkali metal ions include Li, Na, K, Rb, and Cs. We do not observe any significant signal due to the protonated species with any of the sugars in this study. The MALDI of sugars with variable sizes and the use of molecular dynamics calculations allow us to speculate the site of coordination and the number of sugar units involved in these sites.

Experimental Section

The experiments were performed on an external source Fourier transform mass spectrometer built in this laboratory and described in detail in earlier publications (Figure 1).[38,57] The system contains two separate chambers with two external source FTMS instruments. One chamber contains five stages of differential pumping and an electrospray ionization source. The MALDI/FTMS chamber, situated in the opposite side of a 3-T superconducting magnet, contains two stages of differential pumping and a MALDI/LSIMS source. Ions that are formed and extracted from the source are transported to the ion cyclotron resonance (ICR) cell by a set of RF-only quadrupole rods. The rods are used to focus the ions through the fringing field of the magnet, and are not used for mass selection. Differential pumping allows the analyzer cell to be kept as low as 10^{-10} Torr even when a sample is in place in the source. The ions are trapped in an elongated ICR cell ($2 \times 2 \times 4$ in.), which is located in the homogeneous region of a 3-T superconducting magnet (Cryomagnetics, Inc., Oak Ridge, TN). The pulse sequence is controlled by an Omega data system (Ionspec Corp., Irvine, CA). The data system allows for precise control of the trapping potentials, which was critical in trapping the injected ions.

All of the samples analyzed are commercially available (Sigma Chemical Co., St. Louis, MO; Biocarb Chemical, Lund, Sweden; and Oxford Glycosystems, Oxford, UK) and used without further purification. 2,5-Dihydroxybenzoic acid (Aldrich Chemical Co., Milwaukee, WI) was used as the matrix at a concentration of 0.3 M in ethanol. The matrix to analyte molar ratio was typically in the order of 500:1. The samples were prepared in concentrations of 0.5−2.5 mg/mL in methanol. Typically, 1 μL (about 1−5 μg) of sample is applied to the probe tip, followed by 1 μL of 0.01 M dopant and 1 μL of matrix. The probe area is currently relatively large with the laser spot size being less than one-tenth of the total area. This and the observation that up to 100 shots fired on a single spot still gave useful signal means that the total amount of material to obtain the spectra is on the order of 5−25 ng. Modification of the probe tip, so that only a smaller volume

(36) Spengler, B.; Kirsch, D.; Kaufmann, R.; Lemoine, J. *J. Mass Spectrom.* **1995**, *30*, 782−7.
(37) Li, Y. Z.; McIver, R. T., Jr.; Hunter, R. L. *Anal. Chem.* **1994**, *66*, 2077−83.
(38) Fannin, S. T.; Wu, J.; Molinski, T.; Lebrilla, C. B. *Anal. Chem.* **1995**, 67, 3788−92.
(39) McIver, R. T., Jr.; Li, Y. Z.; Hunter, R. L. *Proc. Natl. Acad. Sci. U.S.A.* **1994**, *91*, 4801−5.
(40) Bornsen, K. O.; Mohr, M. D.; Widmer, H. M. *Rapid Commun. Mass Spectrom.* **1995**, *9*, 1031−4.
(41) Ashton, D. S.; Bedell, C. R.; Cooper, D. J.; Lines, A. C. *Anal. Chim. Acta* **1995**, *306*, 43−8.
(42) Whittal, R. M.; Palcic, M. M.; Hindgaul, O.; Li, L. *Anal. Chem.* **1995**, *67*, 3509−14.
(43) Mohr, M. D.; Bornsen, K. O.; Widmer, H. M. *Rapid Commun. Mass Spectrom.* **1995**, *9*, 809−14.
(44) Juhasz, P.; Biemann, K. *Carbohydr. Res.* **1995**, *270*, 131−47.
(45) Harvey, D. J.; Rudd, P. M.; Bateman, R. H.; Bordoli, R. S.; Howes, K.; Hoyes, J. B.; Vickers, R. G. *Org. Mass Spectrom.* **1994**, *29*, 753−66.
(46) Spengler, B.; Kirsch, D.; Kaufmann, R.; Lemoine, J. *Org. Mass Spectrom.* **1994**, *29*, 782−7.
(47) Stahl, B.; Thurl, S.; Zeng, J. R.; Karas, M.; Hillenkamp, F.; Steup, M.; Sawatzi, G. *Anal. Biochem.* **1994**, *223*, 218−26.
(48) Harvey, D. J. *Rapid Commun. Mass Spectrom.* **1993**, *7*, 614−9.
(49) Juhasz, P.; Costello, C. E. *J. Am. Soc. Mass Spectrom.* **1992**, *3*, 785−96.
(50) Ingendoh, A.; Karas, M.; Hillenkamp, F.; Giessmann, U. *Int. J. Mass Spectrom. Ion Processes* **1994**, *131*, 345.
(51) Quist, A. P.; Huth-Fehre, T.; Sundqvist, B. U. R. *Rapid Commun. Mass Spectrom.* **1994**, *8*, 149−54.
(52) Dreisewerd, K.; Schuerenberg, M.; Karas, M.; Hillenkamp, F. *Int. J. Mass Spectrom. Ion Processes* **1995**, *141*, 127.
(53) Mock, K. K.; Davey, M.; Cottrell, J. S. *Biochem. Biophys. Res. Commun.* **1993**, *177*, 644−51.
(54) Karas, M.; Ehring, H.; Nordhoff, E.; Stahl, B.; Strupat, K.; Hillenkamp, F.; Grehl, M.; Krebs, B. *Org. Mass Spectrom.* **1993**, *28*, 1476−81.
(55) Ogier-Denis, E.; Codogno, P.; Chantret, I.; Trugnan, G. *J. Biol. Chem.* **1988**, *263*, 6031−7.
(56) Ogier-Denis, E.; Bauvy, C.; Aubery, M.; Codogno, P.; Sapin, C.; Rousset, M.; Zweibaum, A.; Trugnan, G. *J. Cell. Biochem.* **1989**, *41*, 13.
(57) Gard, E.; Carroll, J.; Green, M. K.; Fannin, S. T.; Wu, J.; Camara, E.; Lebrilla, C. B; The 43rd ASMS Conference on Mass Spectrometry and Allied Topics, Atlanta, GA, 5/21−5/26/95, 1995.

Chart 1

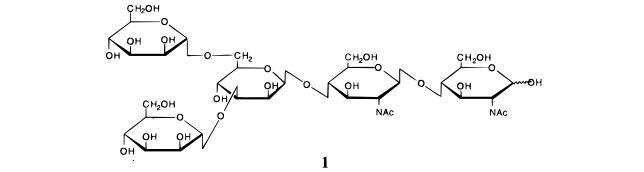

1
Mannose Core

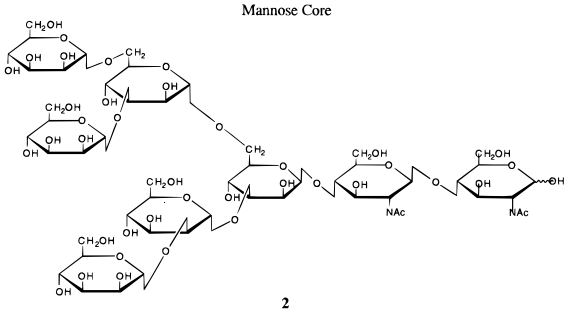

2
$Man_6GlcNAc_2$

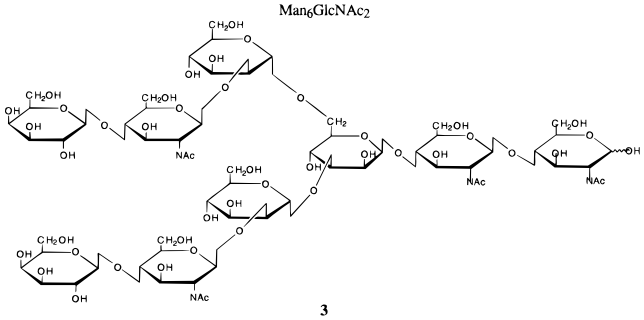

3
$Man_3Gal_2GlcNAc_4$

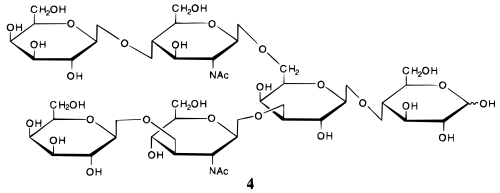

4
Lacto-N-hexoase Core

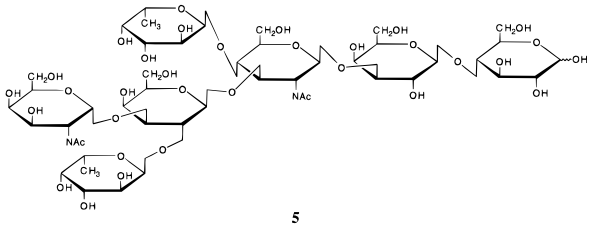

5
A-Heptasaccharide

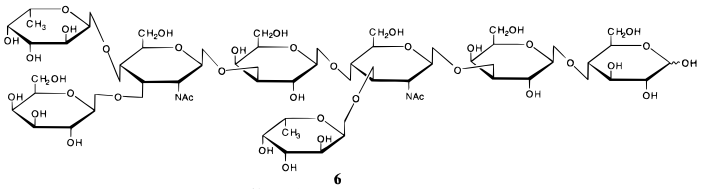

6
Difucosyl-para-lacto-N-hexaose

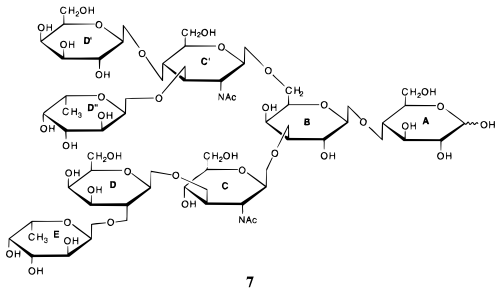

7
Difucosyllacto-N-hexaose-a

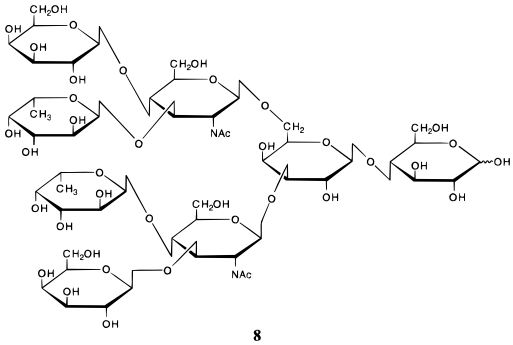

8
Difucosyllacto-N-hexaose-b

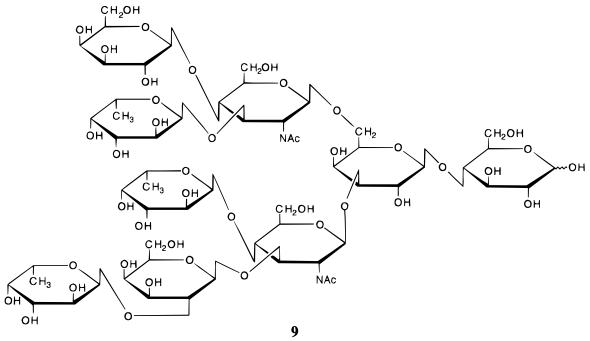

9
Trifucosyllacto-N-hexaose

of sample is actually deposited, will greatly decrease the total amount of material needed for analysis.

Ionization conditions during MALDI were kept constant for all the compounds after initially optimizing for signal yield. Earlier, several investigations on oligosaccharides using liquid secondary ion mass spectrometry (LSIMS) with a Cs^+ source were performed in this laboratory.[20,58,59] We find that the conditions, *i.e.*, electrode potentials, for ion formation and injection for MALDI varied significantly from those used for LSIMS. The extractor potential and the potential at which the quadrupole rods are floated were set substantially less negative compared to LSIMS to achieve adequate ion signal. This may be related to the relatively higher kinetic energy of the ions formed during laser desorption/ionization.[60,61] The pulse sequence used for acquiring signal was modified in order to trap ions formed by MALDI and is adapted from the method described by McIver and co-workers for MALDI of peptides and proteins on a similar instrument.[37] With the front trapping plate set at 0 V and the rear trapping plate set to 10 V, the cooling gas (N_2) is pulsed into the vacuum chamber using a pulsed valve (General Valve Corp., Fairfield, NJ). Nitrogen appears to be the best cooling gas for obtaining optimal ion signal. This may be due to the ability of the pumps to remove nitrogen faster, so that the pressure in the cell is lower when the ions are detected. The ballast pressure and the pulse width of the cooling gas were also important in obtaining good results. Generally, the pressure in the reservoir was about 15−25 Torr and the pulse width used was typically 2 ms. These conditions are naturally highly dependent on the arrangement and volume of the inlet system. The pressure achieved in the vacuum chamber generally peaked at about 8×10^{-5} Torr and pumped back down to the baseline pressure in about 30 s.

After the pulsed gas is introduced into the analyzer chamber, the RF pulse was applied to the quadrupole ion guide. A single laser shot

(58) Carroll, J.; Lebrilla, C. B.; Ngoka, L.; Beggs, C. G. *Anal. Chem.* **1993**, *65*, 1582−7.

(59) Carroll, J.; Willard, D.; Lebrilla, C. B. *Anal. Chim. Acta* **1995**, 431−47.

(60) Woodin, R. L.; Beauchamp, J. L. *Chem. Phys.* **1979**, *4*, 1−9.

(61) Bouchoux, G.; Jezequel, S.; Penaud-Berryuer, F. *Org. Mass Spectrom.* **1993**, *28*, 421−7.

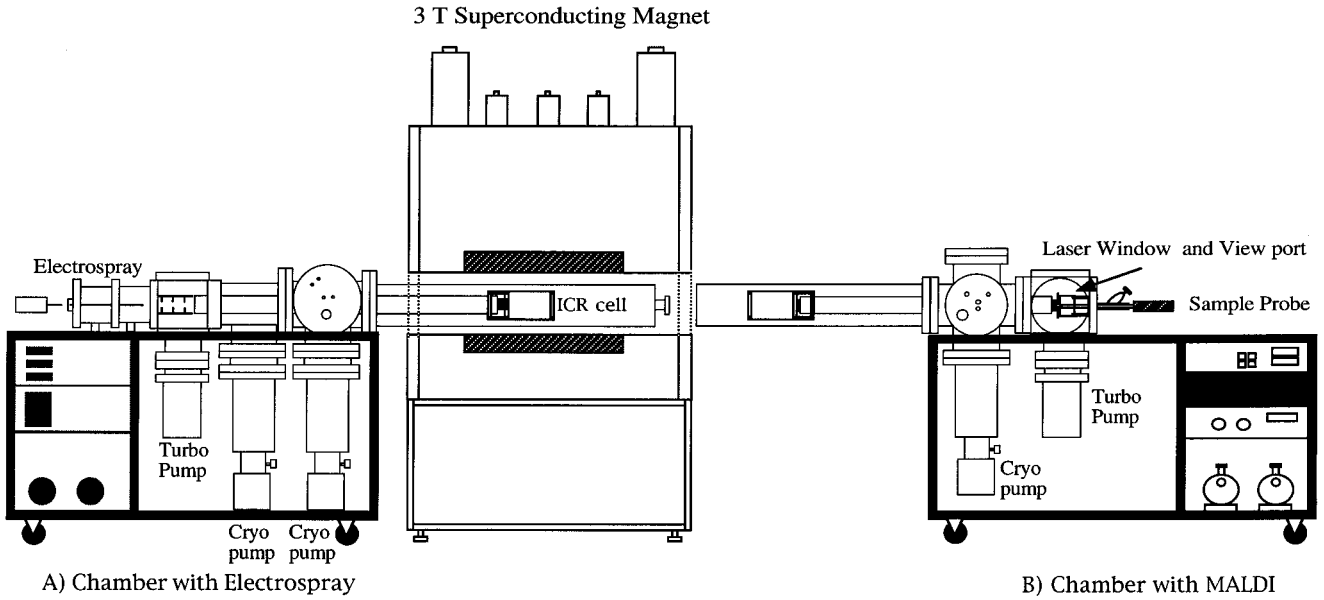

Figure 1. Schematic of the instrument containing both MALDI (Chamber B) and ESI (Chamber A). When MALDI/FTMS is performed the analyzer cell is placed in the bore of a 3-T superconducting magnet and the data system is connected.

was then fired, and the ions were extracted and transported through the quadrupole rods and into the ICR cell. After a short delay, the front trapping plate was gated up to 10 V to keep the ions from leaving the cell. The timing of this pulse is important, as gating the pulse too soon would reflect the ions away from the cell, and gating the plate too late would allow the ions to leave the cell before they are trapped. It is directly related to the quadrupole bias DC voltage. For the results presented, the gating delay time was set to 0.45 ms and the other parameters were optimized to achieve the most intense ion signal. After a cooling period of 10 s, the trapping plate potentials were ramped down to 0.5−1.5 V for ion excitation and subsequent detection. The length of this cooling period is variable, and depends highly on the peak pressure of the pulsed gas. The entire sequence could then be repeated to obtain multiple scans for signal averaging.

Results

High mannose sugars (**1**−**3**) and carbohydrate derivatives from human milk (**4**−**9**) were analyzed with MALDI/FTMS (see Chart 1 for structures). The two classes of sugars are biologically important and provide a hint of the wide variety of carbohydrate structures present in human biology. The compounds were chosen as they varied in size and in degree of branching. MALDI/TOF MS of oligosaccharides from human milk has been performed by Stahl *et al.*[47] The method was shown to be highly effective for mixtures yielding new and yet to be characterized oligosaccharides. However, it provided little or no fragmentation for structural elucidation. Using the method of post-source decay Spengler *et al.* were able to obtain numerous fragment ions corresponding to glycosidic bond and cross-ring cleavages from MALDI produced ions.[36] To obtain spectra with extensive fragmentation and resolving powers of 400−500 (fwhh), several raw spectra were combined.

Unless specified all spectra shown are obtained directly from raw data transferred to a spreadsheet program for presentation. The experiments, unless indicated, are performed under identical tuning conditions. Maintaining the tuning parameters is important for the comparison of fragment ion yields discussed below. In the mass range presented all peaks are isotopically resolved. The large number of spectra and the limited memory storage space forced us to limit the number of data points to 64K per spectra producing a resolution of only 10000−20000 fwhh. Increasing the number of data points to 128 to 256 allowed us to obtain routine resolution of 50000. In the heterodyne mode (narrow band) resolution of 200000 is typically obtained. The inset spectra shown in some of the figures correspond to resolutions of only 10000.

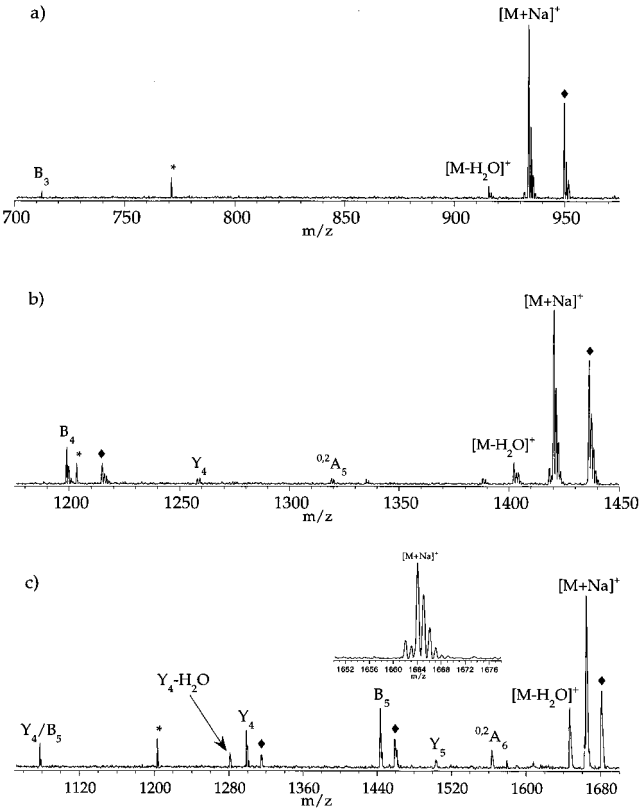

Figure 2. The MALDI/FTMS spectra of (a) mannose core **1**, (b) $Man_6GlcNAc_2$ (**2**), and (c) $Man_3Gal_2GlcNAc_4$ (**3**) obtained with 2,5-dihydrobenzoic acid as matrix. A nitrogen laser with 337 nm was used for desorption. Peaks labeled with diamonds are potassiated species. Peaks labeled with asterisks are noise.

MALDI/FTMS of Mannose-Type Sugars. The MALDI/FTMS spectrum of the mannose core compound (**1**), a pentasaccharide, contains sodium and potassium in its quasimolecular ion (*m*/*z* 934 and 950, respectively, Figure 2a). In nearly every case, the potassiated ion signal is strong. The alkali metal ions probably come from the glass containers used in the

preparation of the sample. The protonated molecule $[M + H]^+$ is not observed using the sample preparation described. Fragmentation in the spectrum is minimal and corresponds to a loss of water (*m/z* 916) and loss of the *N*-acetylglucosamine (GlcNAc) reducing end (*m/z* 712, B_3 according to the Domon−Costello formalism[12] or $[M + Na - GlcNAc]^+$) from the sodiated parent. The cleavage assignments, *e.g.*, B_3, are all tentative assignments and have not been rigorously verified. In each spectrum, only portions that contain signals are presented. In Figure 2a, for example, signals below *m/z* 700 are not observed. Increasing the size of the sugar by three additional mannose to the $Man_6GlcNac_2$ (**2**) produces slightly more fragment ions (Figure 2b). The sodiated and potassiated parents remain the dominant peaks in the spectrum (*m/z* 1420, 1436) with the loss of the reducing end from both Na^+ and K^+ quasimolecular ions being the most abundant fragment ions (*m/z* 1199, B_4). Cross-ring cleavage of the reducing end is observed producing losses of carbons 1 and 2 (*m/z* 1320, $^{0,2}A_5$ fragment). A loss of one of the nonreducing sugars is also observed producing the corresponding sodiated (*m/z* 1258, Y_4) species. The nonasaccharide $Man_3Gal_2GlcNAc_4$ (**3**) produces significantly more fragment ions (Figure 2c). Both the number of fragment ions of **3** and their total intensity in the MALDI/FTMS spectrum are greater than those of both **1** and **2**. The fragment ions correspond to similar cleavages, however, with the most intense peak corresponding to the loss of the reducing end sugar and loss of water (*m/z* 1443 or B_5 and *m/z* 1646 or $[M + Na - H_2O]^+$, respectively). Other abundant fragment ion signals correspond to losses of the nonreducing end (*m/z* 1298, Y_4) as well as combinations of multiple glycosidic bond cleavage (*m/z* 1078, Y_4/B_5). It is interesting to note that cross-ring cleavages are observed under MALDI for only the reducing end of compounds **1**, **2**, and **3**. Similar observations have previously been reported.[30]

MALDI/FTMS of Oligosaccharides Derived from Human Milk. The core compound (lacto-*N*-hexaose, **4**) shows moderate fragmentation corresponding to glycosidic bond cleavages Y_2 (*m/z* 730), Y_3 (*m/z* 934), and B_3 (*m/z* 915) (Figure 3a). The quasimolecular ion is predominantly the sodiated species (*m/z* 1096) with some potassiated species (*m/z* 1112) present. Cross-ring cleavages are again observed only at the reducing end (*m/z* 1036, $^{0,2}A_4$ and *m/z* 975, $^{2,4}A_4$), although *m/z* 975 could also be fragmentation at the nonreducing end ($^{0,2}X_3$).

A slightly larger compound with two fucosyl sugars branched off the main sequence is A-heptasaccharide (**5**). The MALDI/FTMS spectrum shows a predominant quasimolecular ion ($[M + Na]^+$, *m/z* 1226). Fragmentation is more extensive relative to the core compound with the dominant fragment ions corresponding to glycosidic bond cleavages. The most abundant is loss of one fucose group (*m/z* 1080, $Y_{3\beta}$ or $Y_{4\alpha''}$); the next most abundant are the losses of one GlcNAc and cross-ring cleavage (*m/z* 1022, $Y_{4\alpha'}$ and *m/z* 1166, $^{0,2}A_5$, respectively). The losses of two fucose groups is also observed (*m/z* 934). Cross-ring cleavages are also observed primarily on the reducing ring (*m/z* 1166, $^{0,2}A_5$ and *m/z* 1106, $^{2,4}A_5$ or $^{0,2}X_{4\alpha''}$) (Figure 3b).

Three octasaccharide isomers each containing two fucosyl groups were analyzed by MALDI/FTMS. The fucosyl sugars are generally labile with the loss of one being the most abundant fragment ion. One compound (difucosyl-*p*-lacto-*N*-hexaose, **6**) produced the greatest amount of fragmentation (Figure 4a). Loss of a fucose (*m/z* 1242, $Y_{3\beta}$ or $Y_{5\alpha''}$) from the sodiated parent ($[M + Na]^+$ *m/z* 1388) produced a signal with an intensity greater than the quasimolecular ion. The loss of the second fucose ($Y_{5\alpha''}/Y_{3\beta}$ *m/z* 1095) is about 20% as intense. Other glycosidic bond cleavage products are observed such as *m/z*

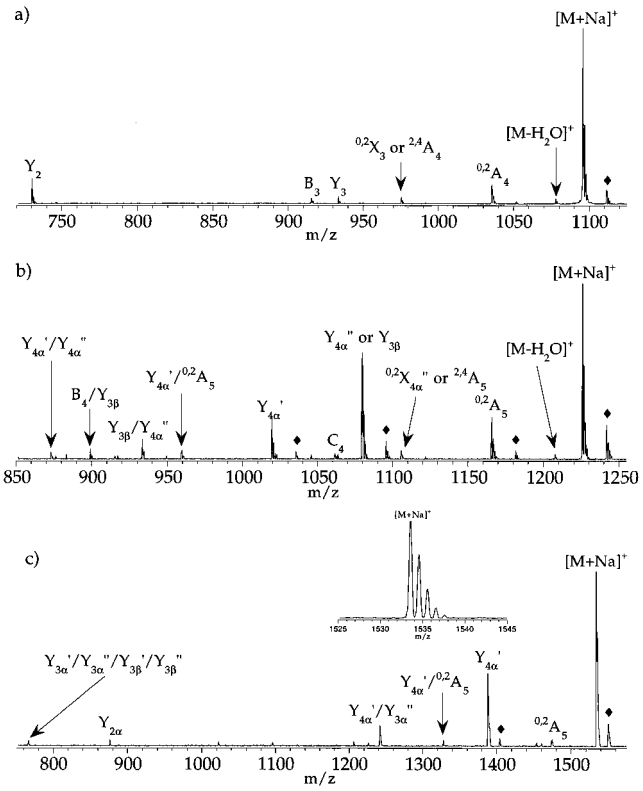

Figure 3. The MALDI/FTMS spectra of (a) lacto-*N*-hexaose (**4**), (b) A-heptasaccharide (**5**), and (c) trifucosyllacto-*N*-hexaose (**9**) derived from human milk. Peaks labeled with diamonds are potassiated species. Peaks labeled with asterisks are noise.

1046 (B_4) and combinations of glycosidic bond cleavages such as *m/z* 900 ($B_5/Y_{5\alpha'}/Y_{5\alpha''}$) and *m/z* 754 corresponding to $B_4/Y_{3\beta}/Y_{5\alpha''}$. An isomer that is more highly branched but also contains two fucosyl groups is difucosyllacto-*N*-hexaose-*a* (**7**). The amount of fragmentation is considerably less than that for **6** (Figure 4b). The sodiated parent is the most abundant ion (*m/z* 1388) with the loss of fucose ($Y_{4\alpha}$ or $Y_{3\beta''}$) being the most abundant fragment ion (*m/z* 1242, 28%). The loss of a second fucose is similarly considerably reduced ($Y_{4\alpha}/Y_{3\beta''}$, *m/z* 1095, 6%). The remaining fragment ions have relatively weak abundances (<5%) but are still structurally informative, including *m/z* 1226, $Y_{3\beta'}$. The major cross-ring cleavage observed again occurs on the reducing ring (*m/z* 1328, $^{0,2}A_5$). The other highly branched isomer (difucosyllacto-*N*-hexaose, **8**) also produces considerably fewer fragment ions (Figure 4c). The fragment ions produced are similar to those obtained with **7**. Differentiation of **7** and **8** by mass spectrometry would be extremely difficult.

The MALDI/FTMS spectra of the highly branched nonasaccharide trifucosyllacto-*N*-hexaose (**9**) contains the sodiated parent as the base peak with again loss of one fucosyl group as the major fragment ion ($Y_{4\alpha'}$ or $Y_{3\alpha''}$, *m/z* 1388, Figure 3c). The loss of two fucosyl is also abundant ($Y_{4\alpha'}/Y_{3\alpha''}$, *m/z* 1242); however, loss of three fucosyl groups (*m/z* 1096) is weak. The only other fragment ion observed corresponds to cross-ring cleavage of the reducing ring ($^{0,2}A_5$, *m/z* 1474).

Branching and Fragment Ion Yield. While there appears to be little correlation between fragment ion yield and structure, closer inspection of all the spectra reveals that there is a relationship between oligosaccharide branching and fragment ion yield. Under similar tuning conditions with which the spectra were obtained, linear oligosaccharides fragment more than those that are branched. The MALDI/FTMS spectrum of the linear pentasaccharide, maltopentaose, contains a greater

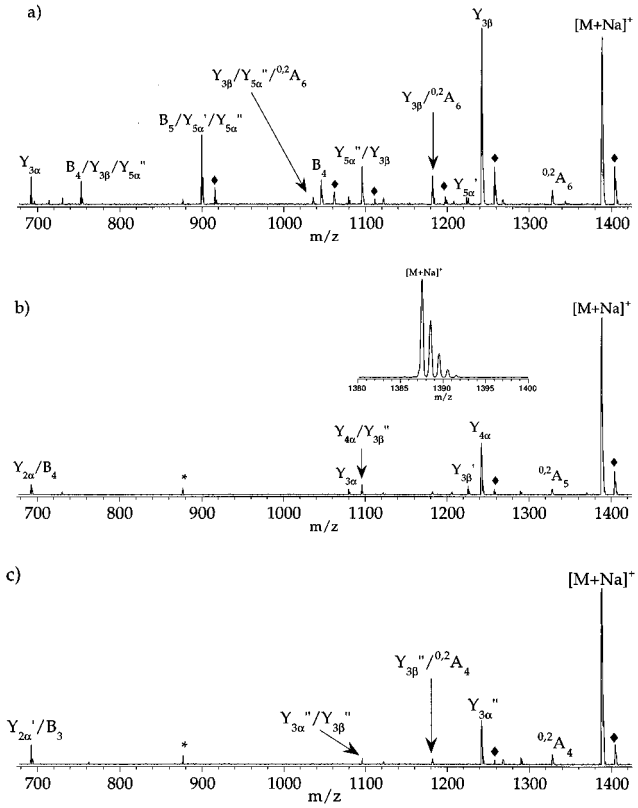

Figure 4. The MALDI/FTMS spectra of (a) difucosyl-*p*-lacto-*N*-hexaose (**6**), (b) difucosyllacto-*N*-hexaose-*a* (**7**), and (c) difucosyllacto-*N*-hexaose-*b* (**8**) derived from human milk. Peaks labeled with diamonds are potassiated species. Peaks labeled with asterisks are noise.

amount of fragment ions (72% relative abundance, not shown) than the highly branched pentasaccharide **1** (<10%). The effect is also apparent in the MALDI/FTMS of the three isomeric octasaccharides from human milk. The highly branched isomers **7** and **8** have smaller amounts of fragment ions in their respective MALDI/FTMS spectra than the less branched isomer **6**.

To determine whether this behavior is general, it became necessary to determine the degree of fragmentation as a function of branching. Assigning how much a compound is branched can be made somewhat objectively, but direct comparisons between compounds would be greatly simplified by assigning a numerical value to a certain degree of branching. We are not aware of any published method that assigns a branching number to oligosaccharides. However, the capability to correlate branching to fragment ion yield has very important analytical application and could provide additional structural information. For example, isomers can be determined to be more or less branched relative to some known structure from the relative amount of fragment ions observed in the MALDI/FTMS spectra.

A formula was devised to assign a degree of branching (B_D) to an oligosaccharide based on the longest continuous linear chain containing the reducing end and various weights to side chains. Side chains are categorized depending on whether they are attached to the main linear unit or to some other side chains. The side chain has a higher value the further it is from the main chain. The size of the side chain is also important and is given by the number of saccharide monomers on the particular side chain; the size of the side chain adds to the degree of branching. The size of the compound is considered to allow comparisons between oligosaccharides containing different numbers of monomers. It serves to normalize the number so that large

Scheme 1

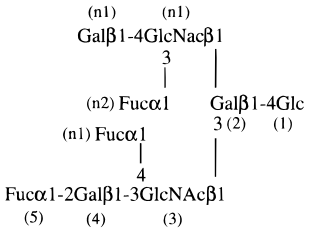

Table 1. Percent of Fragment Ion Abundances and Degree of Branching for Oligosaccharides Examined in This Report

oligosaccharide	fragmentation (%)	B_D
difuco-*p*-lacto-*N*-hexaose (**6**)	75.2	0.14
A-heptasaccharide (**5**)	59.2	0.17
$(Man)_3(Gal)_2(GlcNAc)_4$ (**3**)	57.3	0.20
difucosyllacto-*N*-hexaose-*a* (**7**)	37.7	0.31
$(Man)_6(GlcNAc)_2$ (**2**)	35.3	0.31
triflucosyllacto-*N*-hexaose (**9**)	44.4	0.36
difucosyllacto-*N*-hexaose-*b* (**8**)	34.3	0.42

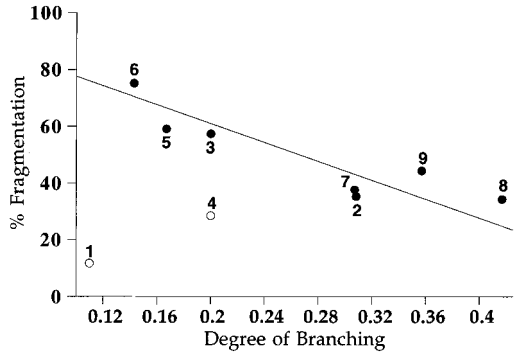

Figure 5. Plot of degree of branching (B_D) versus percent fragmentation for the seven oligosaccharides. The two core compounds **1** and **4** were removed from the correlation ($R = 0.90$).

compounds will not necessarily always have a high degree of branching. The size of the longest continuous chain is also included for similar reasons. The full equation is given as:

$$B_D = \frac{(1\sum n_1) + (2\sum n_2) + (3\sum n_3)...}{T + L}$$

where B_D = degree of branching, T = total number of monomer units, L = number of units in the longest, least-branched, continuous chain containing the reducing end, n_1 = number of units in all primary antennae connected to the primary chain (L), and n_2 = number of units in secondary antennae.

The calculation is illustrated with trifucosyllacto-*N*-hexaose, **9**. The total number of units (T) is 9 (Scheme 1). The longest length (L) has 5 units. There are three primary branch (n_1) and one secondary branch (n_2) units. From the formula a degree of branching is calculated corresponding to

$$B_D = \frac{(1 \times 3) + (2 \times 1)}{9 + 5} = 0.357$$

Table 1 summarizes the B_D and percent fragmentation for seven of the sugars used in the study. The sugars are listed in order of increasing B_D. There is a general correlation between B_D and fragment ion yield with the most highly branched producing the least amount of fragment ions. A plot of the B_D versus percent fragmentation shows this linear behavior clearly (Figure 5). The values in Table 1 are the filled circles and a linear correlation of 0.90 is obtained.

Table 2. Percent of Fragment Ion Abundances and Degree of Branching for the Two Core Compounds

oligosaccharide	fragmentation (%)	B_D
(**1**) mannose core	11.7	0.11
(**4**) lacto-*N*-hexaose core	28.5	0.20

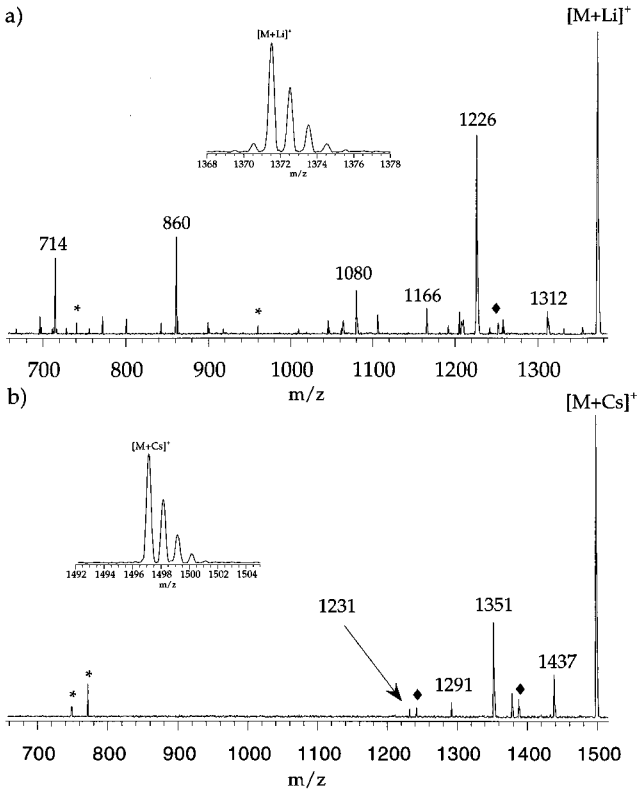

Figure 6. The MALDI/FTMS spectra of difucosyllacto-*N*-hexaose-*b* (**8**) with the sampled doped with LiCl (a) and CsCl (b). Peaks labeled with diamonds are potassiated species. Peaks labeled with asterisks are noise.

The two core compounds, mannose core (**1**) and lacto-*N*-hexaose core (**4**) are not included in the correlation as they do not fall within this general behavior (open circles, Figure 5). The fragment ion abundance of the core compounds is significantly less (Table 2), much less than that predicted given the degree of branching, implying a specific intrinsic stability associated with these structures. The apparent reason for the stability will be discussed further below.

Alkali Metal Ion Size and Fragment Ion Yield. All MALDI/FTMS oligosaccharide spectra discussed so far contain the sodiated parents as the most abundant quasimolecular ions even when the sample is not doped with alkali metal salts. The relationship between branching and fragment ion yield probably stems from the specific coordination of the sodium ion to the compound. Varying the size of the metal ion should further affect the amount of fragment ions formed during MALDI. When 1 μL of sample **8** (8×10^{-4} M) is co-applied on the probe tip with 1 μL of a LiCl solution (0.01 M), the lithiated parent becomes the major quasimolecular ion in the spectra. When the lithiated species is the most abundant quasimolecular ion, we observe a significant increase in the number and relative abundances of fragment ions. For example, the MALDI/FTMS of **8** doped with LiCl show significantly more fragment ions (Figure 6a) than those not doped (Figure 4c) or doped with NaCl. Loss of one (*m*/*z* 1226, $Y_{4\alpha}$ or $Y_{3\beta''}$) and two (*m*/*z* 1080, $Y_{4\alpha}/Y_{3\beta''}$) fucose units is markedly enhanced. In addition, fragment ions corresponding to other glycosidic bond cleavages such as $Y_{2\beta}$ or $Y_{2\alpha}$ (*m*/*z* 860) and combinations (e.g. *m*/*z* 714, $Y_{2\alpha}/Y_{3\beta''}$ or $Y_{2\beta}/Y_{3\alpha''}$) are readily observed. Smaller abundances are observed for cross-ring cleavage at the reducing end (*m*/*z* 1312, $^{0,2}A_4$) and for numerous combinations of glycosidic bond cleavages and cross-ring cleavages such as *m*/*z* 1166 ($^{0,2}A_4$ = loss of fucose). Many of the weaker signals are other combinations of the cleavages described.

Table 3. Structural Assignments of Difucosyllacto-N-hexaose with Masses Derived from Figure 6a and 6b

fragment ion	*m*/*z* Li adduct	*m*/*z* Cs adduct
$^{0,2}A_4$	1312	1437
$^{0,2}X_{3\alpha'}$	1521	1377
$Y_{3\beta''}$	1226	1351
$Y_{3\beta'}$	1210	
B_3	1192	
$Y_{3\beta''}/^{0,2}A_4$	1166	1291
$Y_{3\beta''}/^{0,2}X_{3a'}$	1106	1231
$Y_{3\alpha''}/Y_{3\alpha''}$	1080	
$Y_{3\beta''}/Y_{3\beta'}$	1064	
$Y_{3\beta'}/B3$	1045	
$Y_{3\beta''}/Y_{3\beta'}/Y_{3\alpha''}$	899	
$Y_{2\alpha}$	860	
$Y_{2\alpha}-H_2O$	842	
$Y_{2\alpha}/^{0,2}A_4$	800	
$Y_{2\alpha}/Y_{3a''}$	714	
$Y_{2\alpha}/B_3$	696	

Table 4. Percent of Fragment Ion Abundances with Various Alkali Metal Ions In MALDI/FTMS of Two Oligosaccharides

oligosaccharide	Li^+	Na^+	K^+	Rb^+	Cs^+
6	91	85	85	68	52
8	66	52	*a*	*a*	39

[a] Experiment not performed.

When compound **8** is doped with CsCl (0.01 M), the amount of fragment ions decreases significantly, relative to both lithiated and sodiated samples (Figure 6b). The loss of one fucose remains the major fragment ion (*m*/*z* 1351); however, loss of two fucose is not observed. The only fragment ions due to cross-ring cleavages similarly correspond to $^{0,2}A_4$ (*m*/*z* 1437) and $Y_{3\beta''}/^{0,2}A_4$ (*m*/*z* 1291). A summary of the proposed cleavages and masses is presented in Table 3.

The relationship between poor fragmentation and increasing alkali metal ion size is a general one and is observed when **6** and **8**, two compounds with different fragmentation behavior, are doped with salts of Li, Na, K, Rb, and Cs (Table 4). The trend is readily apparent: with increasing alkali metal ion size, the amount of fragment ions decreases for both compounds. Lithium produces the greatest amount of fragment ions (91% for **6** and 66% for **8**) and cesium the least (52% for **6** and 39% for **8**). Comparison of the amount of fragment ions for **6** and **8** with various alkali metal ions further shows that the other relationship, *i.e.*, between oligosaccharide branching and fragment ion yield, is maintained. In every case, the percent of fragment ions is greater for the more linear **6** than for the more highly branched **8**.

To investigate further the role of the alkali metal ions in the production of fragment ions, a systematic investigation was performed where both the size of the alkali metal ions and the oligosaccharides were varied. Linear oligosaccharides based on maltose (maltose, maltotriose, through maltohexaose) were used. Experiments were performed by doping each compound separately with each of the alkali metal salts (LiCl, NaCl, KCl, RbCl, and CsCl). As discussed earlier, the sodiated parent is observed when no dopant is used and probably originates from the glassware and the matrix. With addition of the appropriate amount of dopant, the respective alkali metal coordinated species of some oligosaccharides are observed. Often, the concentration

Table 5. Minimum Number of Saccharide Units in Carbohydrate Needed to Observe Quasimolecular Ions in Appreciable Amounts (Monosaccharides Were Not Analyzed)

alkali metal	Li	Na	K	Rb	Cs
monomer units needed to observe quasimolecular ion	2	2	3	4	5

Table 6. The Percent of Fragmentation in MALDI/FTMS of Linear Oligosaccharides Derived from Maltose

	percent fragmentation as function of coordinated metal ion				
sugar	Li	Na	K	Rb	Cs
maltose	28	0	NO[a]	NO[a]	NO[a]
triose	66	33	14	NO[a]	NO[a]
tetraose	83	35	6	0	NO[a]
pentaose	89	72	11	0	0
hexaose	55	37	28	9	3

[a] NO = quasimolecular ion not observed under ionization conditions.

of the alkali metal salts had to be varied for individual compounds to find the optimal concentrations for producing quasimolecular ions. Nonetheless, we found that for some oligosaccharides the alkali metal coordinated species is not observed in any appreciable abundances regardless of the concentration of salt. The MALDI/FTMS of lithium and sodium doped samples produced the respective parent as the base peak for all the compounds in the series. Quasimolecular ions were not observed in appreciable abundances for the larger alkali metal ions (K^+, Rb^+, and Cs^+) with the disaccharide maltose. The maltose sample doped with K^+, Rb^+, and Cs^+ produced mainly the sodiated parent even when only a trace amount of Na^+ is present. Large alkali metal ions require larger oligosaccharides to produce the quasimolecular ions. The trisaccharide maltotriose is the smallest sugar that coordinates with K^+ to produce a quasimolecular ion; however, quasimolecular ions of Rb^+ and Cs^+ are not observed (relative abundance <5%) with maltotriose. The quasimolecular ion of Rb^+ is observed only with oligosaccharide at least as large as maltotetraose, while the quasimolecular ion of Cs^+ is observed only with sugars at least as large as maltopentaose (Table 5).

The degree of fragmentation for the linear oligosaccharides also varies considerably with the alkali metal ion. Shown in Table 6 is the percent yield of fragment ions for the linear oligosaccharides as a function of the alkali metal. The degree of fragmentation decreases with increasing alkali metal ion size for every oligosaccharide. For example, pentaose, the smallest linear oligosaccharide with which all the alkali metals produce quasimolecular ions, yields the greatest amount of fragment ions with Li^+ (89%). The amount of fragment ions decreases rapidly with increasing alkali metal ion size (Na^+ 72%, K^+ 11%, Rb^+ 0%, and Cs^+ 0%). Furthermore, when Tables 5 and 6 are compared, one observes that for Na^+, K^+, Rb^+, and Cs^+ the smallest sugars that effectively coordinates the metal ion, to produce quasimolecular ions, yield the least amount of fragment ions. This suggests that charge remote fragmentation is the likely mode of dissociation for oligosaccharides coordinated to these metal ions.

Molecular Modeling and Molecular Dynamics Calculations. The fragmentation behavior of the branched oligosaccharides and the dependency between molecular and metal ion size in the formation of quasimolecular ions reveal useful information concerning the coordination of oligossaccharides to metal ions. It further provides a unique opportunity to assess the utility of molecular modeling programs for these systems. Molecular mechanics and molecular dynamics calculations employing the Amber Force Field in the software Insight II (Biosym Technologies, San Diego, CA) were performed on several oligosaccharide−metal ion systems. Molecular modeling was achieved by starting with an initial guess and heating the molecule to 1000 K. The molecule was annealed by decreasing the temperature gradually (in steps of 100 K) to room temperature where full optimization is performed.

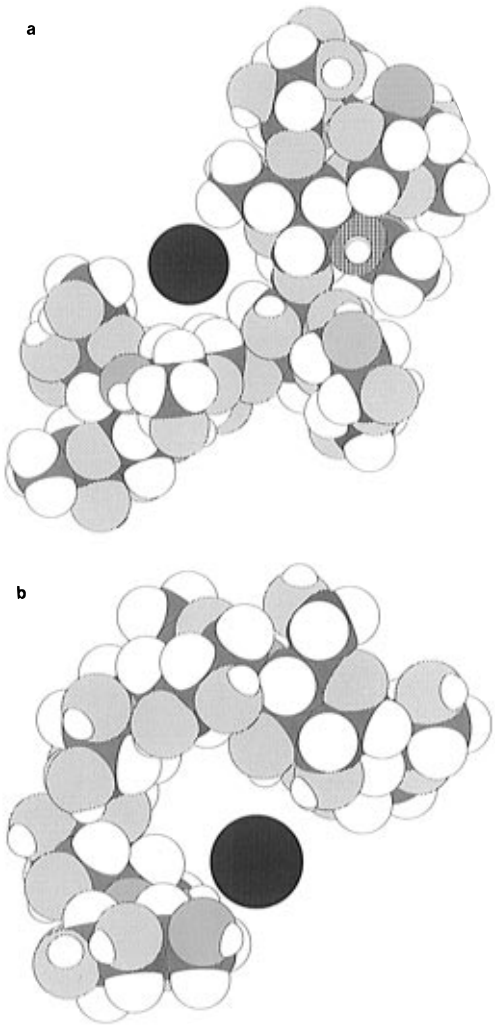

Figure 7. Molecular mechanics calculations of Cs^+ coordinated (a) difucosyllacto-*N*-hexaose-*a* (**7**) and (b) maltohexaose obtained with Insight II. Structures are obtained from 20 heating and annealing cycles. The metal ion is shaded in black. Carbon atoms are shaded gray, oxygen atoms are shaded with diagonal lines, the nitrogen atom is cross-hatched, and hydrogen atoms are not shaded. The relative position of the metal ion did not change between the cycles.

Figure 7a shows a representative structure of Cs^+ coordinated to a highly branched sugar **7** after 20 heating and annealing cycles. We find only small variations in the relative position of Cs^+ after each annealing cycle. The metal ion appears to remain fixed near the major branch point. Careful visual inspection of Cs−O bond distances in Figure 7a indicates that the coordination of Cs^+ involves at least five pyranose rings including A, B, C, C′, and D′ (see structure **7**, Chart 1 ring labels).

Calculations performed with the linear oligosaccharide, maltohexaose, yield similar behavior, producing a complex with multiple coordination between the metal ion and the sugar (Figure 7b). The Cs^+ again appears coordinated to five pyranose rings leaving one free. Unlike linear peptides that can undergo extensive coordination with the alkali metal ion, oligosaccharides are limited by their structure. The presence of the pyranose rings prohibits extensive interactions that would fully envelop

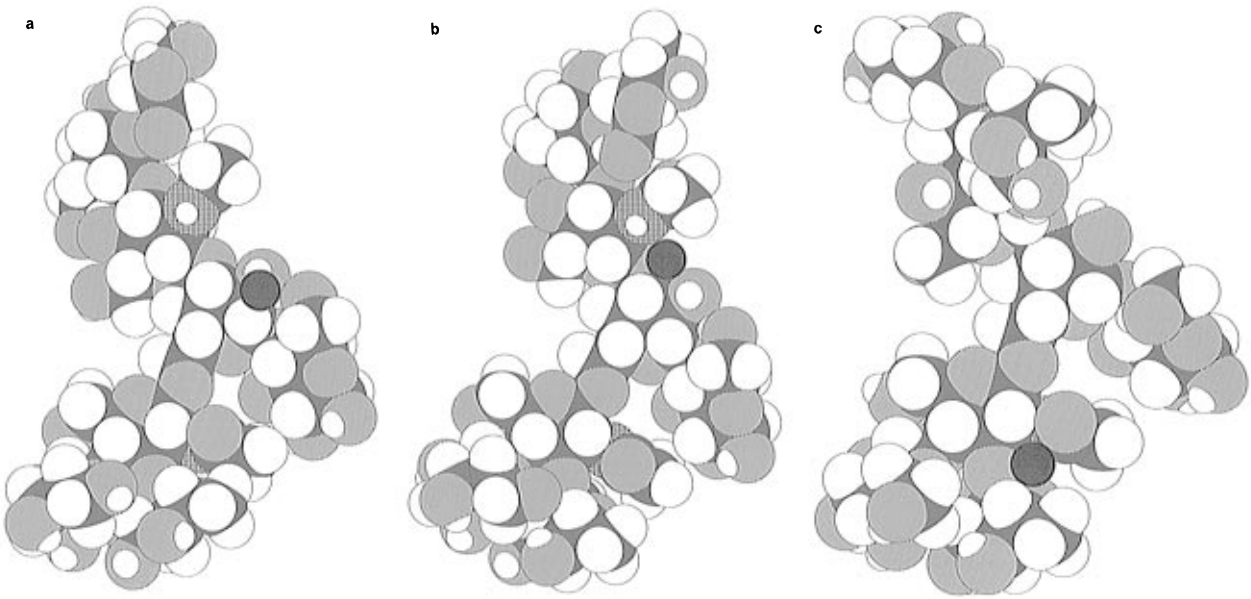

Figure 8. Three representative structures of Li^+ coordinated to difucosyllacto-*N*-hexaose-*a* (**7**) obtained from Insight II using Amber force fields. Structures are representative of several heating (1000 K) and annealing cycles. The relative position of the Li^+ changed with each cycle.

the metal ion. The most compact forms of neutral linear oligosaccharides are helical. The coordination of the metal ion appears to involve insertion of the metal into the rings of the helix. The coordination predicted by these calculations is, however, evidently supported by the experiments, as maltopentaose is the smallest oligosaccharide observed to form the quasimolecular ion with Cs^+. Furthermore, no fragment ions are observed when a maltopentaose sample is doped with CsCl while a hexaose sample similarly doped produces fragment ions, albeit in small abundance.

For comparison, similar calculations were also performed with Li^+, the smallest metal ion of the study. Heating the metal-coordinated oligosaccharide (**7**) to 1000 K causes the Li^+ cation to be mobile moving from one glycosidic bond to another (Figure 8a,b,c,). Its preferred site of coordination is near the glycosidic bond consistent with the results of semiempirical calculations on model disaccharides.[16,62] Coordination of the lithium ion appears to involve only two monosaccharide units, consistent with its size dependency for forming the quasimolecular ion. Its labile nature is also consistent with the fragmentation behavior in the MALDI/FTMS of lithiated **7**. Many fragment ions are the result of combinations of glycosidic bond cleavages which are not observed as frequently with other alkali metal ions, not even with Na^+. Multiple cleavages are possibly due to a mobile lithium atom causing the site of cleavage to correlate, though not necessarily coincide, with the site of coordination.

Discussion

Molecular mechanics calculations and experimental results both indicate that a minimum number of oligosaccharides is necessary to stabilize a specific alkali metal ion complex. For Na^+ and Li^+, two saccharide units are necessary to produce a quasimolecular ion. For K^+, at least three monosaccharides are needed, four for Rb^+ and five for Cs^+. The individual $M^+\cdots O-$ (M = alkali metal) interaction is significantly stronger for the smaller metal ion (Li and Na) than for the large metal ions (Rb and Cs)[20] necessitating a significantly greater number of coordination for the large metal ions to produce a stable complex under MALDI conditions. For large metal ions such as Rb^+ and Cs^+, abundant quasimolecular ions can be achieved with little or no fragmentation. The smallest abundances of fragment ions are obtained when the optimal number of saccharide monomers are attached to the metal ion. For example, Rb^+ doped tetraose and pentaose produce essentially no fragment ions. Fragment ions are observed only when Rb^+ is coordinated to maltohexaose. A Cs^+ doped maltopentaose and maltohexaose produce little or no fragment ions. Additionally, the relationship between fragment ion yield and metal ion size was earlier observed by Fura *et al.*[63] When oligosaccharides were coordinated to Mg^{2+} and Ca^{2+} in an electrospary source and collisionally dissociated, the yield of fragment ions was found greater for the smaller metal. We attribute the lack of fragment ions wit the larger metals to the inability of the metal complex to undergo charge-induced fragmentation. Instead, the complex probably dissociates through charge remote fragmentation.

Metastable dissociation rates of cationized oligosaccharides produced by LSIMS decrease uniformly when the size of the cation is increased from H^+ to Cs^+.[20] Given the results presented here and those obtained by LSIMS, it appears likely that H^+ and Cs^+ coordinated oligosaccharides undergo two very different mechanisms of fragmentation. Protonated species undergo charge-induced cleavages while cessiated species undergo charge-remote fragmentation. The differences in their behavior may be attributed to several factors including the internal energy of the nascent quasimolecular ion and the dissociation barrier toward dissociation. Extensive gas-phase reactions are proposed to occur during both FAB and MALD ionization.[64−66] In the MALDI-FTMS experiments all ions are trapped by a pulsed gas which also serves to thermalize the ions. Trapping ions in FAB-FTMS does not require pulsed gas and the quasimolecular ions are known to contain sufficient energies to dissociate. Unfortunately, the several competing reactions occurring during ionization and the unknown thermochemistry of proton and alkali metal ion binding to oligosaccharides make it difficult to speculate on the effect of internal energy to the fragment ion yield. However, we can speculate

(62) Hofmeister, G. E.; Zhou, Z.; Leary, J. A. *J. Am. Chem. Soc.* **1991**, *113*, 5964−70.
(63) Fura, A.; Leary, J. A. *Anal. Chem.* **1993**, *65*, 2805−11.
(64) Cooks, R. G.; Busch, K. L. *Int. J. Mass Spectrom. Ion Processes* **1988**, *53*, 111−24.
(65) Pachuta, S. J.; Cooks, R. G. *Chem. Rev.* **1987**, *87*, 647−69.
(66) Wang, B. H.; Dreisewerd, K.; Bahr, U.; Karas, M.; Hillenkamp, F. *J. Am. Soc. Mass Spectrom.* **1993**, *4*, 393−8.

Scheme 2

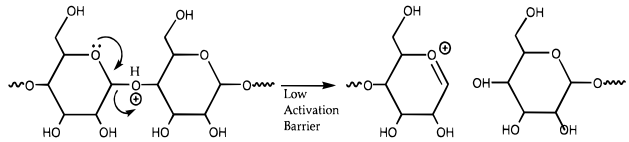

Scheme 3

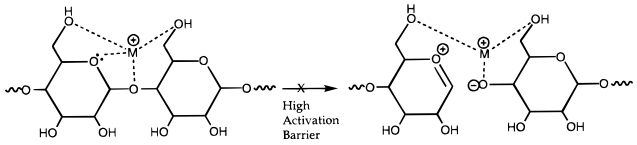

on the affect of barrier height to fragment ion yield. Protons are known to facilitate glycosidic bond cleavages in the gas phase and in solution.[20,67,68] Protons can directly coordinate with at most two oxygen atoms effectively, while alkali metal ions can coordinate to significantly more. Furthermore, the most favorable interaction for protons is where the O···H···O angle is nearly linear. Structural constraints may, therefore, prohibit the proton from coordinating with both oxygens of the hemiketal (the ring and glycosidic bond oxygens) simultaneously. Coordination of the proton on the glycosidic bond is still favorable as this oxygen is the most basic in the molecule. Protonation at this site would produce glycosidic bond cleavage as it allows the ring oxygen to delocalize its electron as shown (Scheme 2).

Alkali metal ions, can undergo coordination with several oxygen atoms simultaneously.[16,69] For example, in Scheme 3 where its position is analogous to the proton in Scheme 2, it is shown coordinated with the glycosidic, ring, and methylene (on the 6 position of the monomer) oxygens. However, coordination of the metal ion to ring oxygen localizes the oxygens' electrons. When it occurs on the ring oxygen, it may prohibit glycosidic bond cleavages (Scheme 3). Therefore, rather than destabilizing, the presence of the alkali metal ion may instead be stabilizing. However, the decreasing rates of metastable dissociation observed in the LSIMS of oligosacchardies may indicate that all other alkali metal ions behave intermediate to H^+ and Cs^+, making charge-remote and charge-induced fragmentation, in certain situations, competitive pathways. For Li^+, for example, large amounts of fragment ions are observed even with the disaccharide maltose suggesting that Li^+ may promote charge-induced dissociation to a high degree. The consequence of this and the possible high mobility of the metal ion is that during ionization the atom moves around the molecular surface promoting cleavages at various points and producing fragment ions derived from multiple cleavage reactions as observed in the MALDI/FTMS spectra of lithium-doped oligosaccharides.

The greater intrinsic stability of highly branched oligosaccharides is likely related to the preference of the alkali metal ion, primarily sodium, to coordinate at or near a branch site. Unlike H^+ and Li^+, Na^+ behaves probably more akin to Cs^+ by not promoting glycosidic bond cleavages. The coordination of Cs^+ to **7** as predicted by molecular modeling is highly consistent with the fragmentation behavior under MALDI/FTMS. The spectrum of **7** doped with CsCl shows the loss of a single fucose group as the major fragment ion, presumably the fucose that is far from the metal ion (Figure 7b). Cross-ring cleavage of the reducing ring A is also observed. This ring is often coordinated to the metal ion via the hydroxyl on carbon-6. This coordination would not hinder cross-ring cleavage as the reaction involves primarily carbon-1 and carbon-2. The coordination of sodium at the branch site also stabilizes the quasimolecular ion as it allows each unit to be in close proximity to the metal. Highly branched compounds are more efficiently coordinated than linear ones. The two core compounds (**1** and **4**) are, therefore, the most highly efficient at coordinating metal ions making them very stable under MALDI/FTMS conditions. We may assume that the coordination of these compounds in solution by alkali metal ions similarly makes them considerably more stable than other oligosaccharides because nearly every glycosidic unit is in contact with the alkali metal. It is perhaps because of this high intrinsic stability that these structures have evolved as the core compound of large highly branched oligosaccharides. Linear oligosaccharides have monosaccharide units that can be far from the metal center while a branched oligosaccharide of comparable size has more glycosidic units that can be in direct contact with the metal ion.

A capability to determine the degree of branching from only the fragment ion yield has direct analytical application in the analysis of oligosacchrides. A numerical scale that assigns a degree of branching will have other important applications. In other analytical techniques such as separations, for example, similar correlation between structure and retention times may be obtained. The linear correlation between branching and fragment ion yield appears to be somewhat general for the small sample presented here.

Acknowledgment. Funds provided by the National Institute of General Medical Sciences, NIH (GM49077-01) are gratefully acknowledged. Several of the oligosaccharides were kindly provided by Prof. Jerry L. Hedricks from the Section of Molecular and Cellular Biology. Computational time has been provided by the Chemistry Department.

JA9603766

(67) Kennedy, J. F.; White, C. A. *Bioactive Carbohydrates*; John Wiley & Sons: New York, 1982.
(68) Gould, R. R., Ed. *Carbohydrates in Solution*; American Chemical Society: Washington, DC, 1971; Vol. 117.
(69) Leary, J. A.; Williams, T. D.; Bott, G. *Rapid Commun. Mass Spectrom.* **1989**, *3*, 192−6.